Toxicology in Vitro 110 (2026) 106151

Contents lists available at ScienceDirect

Toxicology in Vitro

journal homepage: www.elsevier.com/locate/toxinvit

Effects of heated tobacco products and conventional cigarettes on oxidative stress and inflammation in alveolar macrophages

Ok Joo Sul [a,c], Hye Won Choi [a], Seo Hee Park [a,c], Min Ju Kim [a,c], Seung Won Ra [b,c,*]

[a] Biomedical Research Center, Ulsan University Hospital, School of Medicine, University of Ulsan College of Medicine, Ulsan 44033, Republic of Korea
[b] Department of Pulmonary and Critical Care Medicine, Ulsan University Hospital, University of Ulsan College of Medicine, Ulsan 44033, Republic of Korea
[c] Basic-Clinical Convergence Research Institute, University of Ulsan, Ulsan 44610, Republic of Korea

ARTICLE INFO

Editor: Martin Leonard

Keywords:
Chronic obstructive pulmonary disease
Cigarette smoke
Oxidative stress
Inflammation
Autophagy

ABSTRACT

Oxidative stress in macrophages is a major factor contributing to smoking-induced chronic respiratory diseases. However, the oxidative stress induced by heat-not-burn tobacco products (HTP) and conventional cigarettes (3R4F) in macrophages has not been sufficiently investigated. This study compared the effects of HTP and 3R4F cigarettes on cytotoxicity and oxidative stress. We also investigated the underlying mechanisms of autophagy-induced inflammation in macrophages. Our results showed that both HTP and 3R4F cigarette aerosols induced cytotoxicity; however, HTP aerosol was less cytotoxic than conventional cigarette aerosol in RAW264.7 cells. In addition, both aerosols resulted in increased reactive oxygen species (ROS) levels in RAW 264.7 and bone marrow-derived macrophages (BMMs), although the levels were lower for HTP aerosol than for 3R4F aerosol. Additionally, acute exposure to HTP aerosol elevated the levels of IL-1β, IL-6, and TNF-α in macrophages. Oxidative stress-triggered TFEB oxidation induced TFEB nuclear translocation, thereby enhancing autophagy and inflammation in HTP- and 3R4F-exposed macrophages. In conclusion, our study demonstrated that aerosols from HTP and 3R4F cigarettes increased the cytotoxicity in macrophages. Cigarette aerosols increase oxidative stress, which triggers TFEB oxidation and increases its nuclear translocation. TFEB oxidation leads to increased autophagy and inflammation in HTP- or 3R4F aerosol-exposed macrophages. Exposure to HTP aerosols resulted in lower cytotoxicity, oxidative stress, and inflammatory responses than the exposure to conventional cigarettes in vitro.

1. Introduction

Cigarette smoke (CS) is the main etiological factor associated with chronic obstructive pulmonary disease (COPD, Yoshida and Tuder, 2007; Christenson et al., 2022) and cardiovascular diseases (Katanoda and Yako-Suketomo, 2012). COPD is linked to a higher risk of cardiovascular disease and related mortality (Finkelstein et al., 2009). COPD is a progressive and irreversible inflammatory lung disease that leads to limited airflow. Reactive oxygen species (ROS) are responsible for inflammatory responses. CS contains various free radicals and oxidative compounds that can elevate intracellular ROS production in inflammatory and epithelial cells (De Cunto et al., 2018; Joo Sul et al., 2024). CS-induced oxidative stress results in the recruitment of inflammatory cells, primarily alveolar macrophages (AMs) and neutrophils, to the airways, thereby triggering chronic inflammation.

AMs play a crucial role in cytokine production in response to inflammatory stimuli (Hodge et al., 2011). They are linked to the development of lung injury through the initiation of inflammatory reactions. Autophagy is essential for maintaining cellular homeostasis and is crucial for macrophage survival and function. Nevertheless, dysregulation of autophagy has been associated with lung inflammation and the pathogenesis of smoking-related diseases, such as COPD and lung cancer

Abbreviations: AMs, alveolar macrophages; AO, acridine orange; AVOs, acidic vesicular organelles; BALF, bronchoalveolar lavage fluid; BMMs, bone marrow-derived macrophages; COPD, chronic obstructive pulmonary disease; CS, cigarette smoking; ELISA, enzyme-linked immunosorbent assay; H_2DCFDA, 2′,7′-dichlorofluorescein diacetate; HTP, heat-not-burn tobacco product; 3-MA, 3-methyladenine; NAC, *N*-acetyl-l-cysteine; ROS, reactive oxygen species; TFEB, transcription factor EB.

* Corresponding author at: Department of Pulmonary and Critical Care Medicine, Ulsan University Hospital, University of Ulsan College of Medicine, Ulsan 44033, Republic of Korea.
E-mail address: docra@docra.pe.kr (S.W. Ra).

https://doi.org/10.1016/j.tiv.2025.106151
Received 9 June 2025; Received in revised form 11 August 2025; Accepted 20 September 2025
Available online 26 September 2025

(Gouzi et al., 2018; Wang et al., 2018). The mechanism and effects of heat-not-burn tobacco products (HTP) or 3R4F cigarette aerosol-induced autophagy activation on lung inflammation in lung macrophages remain to be elucidated. Understanding the underlying mechanisms of autophagy in response to CS exposure may offer insights into potential therapeutic strategies for mitigating smoking-related health risks. Therefore, animal models and in vitro mechanistic studies are necessary to study the cellular effects of HTP and e-cigarettes, and to better understand the molecular and cellular changes induced by these new products.

HTPs are electronic devices designed to heat rather than burn tobacco, thereby producing aerosols with fewer toxicants than traditional cigarettes (Glantz, 2018). The cytotoxicity and oxidative stress caused by HTP aerosols are significantly lower than those caused by CS (Horinouchi and Miwa, 2021). An increasing number of in vitro studies have highlighted the cytotoxicity of HTP products. Research using NCI-H292 human bronchial epithelial cells showed that HTPs exhibited higher cytotoxicity and cytokine release than e-cigarettes but lower than combustible cigarettes (Leigh et al., 2018). Wang et al. (2024) found that while HTPs may be less harmful than tobacco cigarettes, they demonstrate significant cytotoxicity that increases with dosage in a 3D chip model. In contrast, Dusautoir et al. (2021) revealed that HTPs provoke biological responses in BEAS-2B cells similar to those of combustible cigarettes, unlike e-cigarettes. Further in vitro and animal studies are needed to identify the molecular changes induced by these products. Several studies on lung-derived cells have investigated the effects of heat-not-burn products (HTPs). Exposure to HTPs increases oxidative stress and the production of inflammatory cytokines in pulmonary cell lines (Dusautoir et al., 2021; Sohal et al., 2019). Additionally, alveolar macrophages exposed to HTPs or cigarette smoke demonstrate impaired phagocytosis, with both exposures enhancing the secretion of IL-1β (Scharf et al., 2024). Notably, iQOS exposure significantly reduced glutathione (GSH) levels and increased oxidative stress in alveolar macrophages (Sawa et al., 2022). Overall, HTPs can alter the function and behavior of lung cells, including epithelial cells and macrophages, resulting in increased inflammation. Therefore, in vitro mechanistic studies and animal models are required to identify novel product-induced molecular and cellular changes. In the present study, we investigated how HTP and 3R4F cigarette aerosols elevated oxidative stress-induced inflammation in macrophages. It is well established that oxidative stress can trigger various cellular responses, including the oxidation of TFEB, which promotes its nuclear translocation. This translocation consequently enhances expression of autophagy-related genes. Induction of autophagy has been linked to inflammation. Understanding these mechanisms is crucial for elucidating the effects of aerosol exposure on inflammation and pulmonary health.

In this study, lung macrophages were exposed to HTP (iQOS 3 Duo) aerosol or University of Kentucky reference cigarette (3R4F) smoke. The heating mode of the iQOS 3 Duo operates by using a heating blade to heat the tobacco leaves, generating an aerosol instead of smoke. We compared the cytotoxicity of HTP or CS aerosols in lung macrophages and evaluated the oxidative stress and inflammatory responses induced by them.

2. Materials and methods

2.1. Animal experiments

Ten 6-week-old specific pathogen-free female BALB/c mice weighing 18–20 g were purchased from Koatech Co. (Pyongtaek, Korea). The mice were housed in a specific pathogen-free animal facility and used after one week of acclimatization. All animal procedures were conducted under the "Guide for the Care and Use of Laboratory Animals" (National Research Council US, 2011). This study was reviewed and approved by the Institutional Review Board (IRB) of Ulsan University Hospital (UUH; IRB No. NON2022–002) and Ulsan University Hospital Institutional Animal Care and Use Committee (UIACUC; No. A-211227-03). Female mice were used in this study based on their increased susceptibility to smoke-induced damage and the earlier onset of emphysema in female A/J mice (Gan et al., 2006; Langhammer et al., 2003; March et al., 2006).

2.2. Reagents and antibodies

H_2DCFDA and acridine orange (A1301) were purchased from Invitrogen (Carlsbad, CA). *N*-acetyl-l-cysteine (NAC; A9165), Hoechst 33342 (H3570), Trypan Blue Solution (0.4 %; 15,250,061), 3-methyladenine (3-MA; M9281), and penicillin-streptomycin (P4333) were purchased from Sigma-Aldrich (St. Louis, MO, USA). Fetal bovine serum (FBS, S001–01) and phosphate-buffered saline (PBS, ML008–50) were obtained from Welgene (Daegu, Korea). CellTiter 96TM aqueous one solution cell proliferation assay (MTS; G3580) and Cyto-ID autophagy detection kit 2.0 (ENZKIT175–0050) were purchased from Promega (Madison, WI, USA). N-(Biotinoyl)-N′- (iodoacetyl) ethylenediamine (BIAM; AS-60644) was purchased from AnaSpec (Fremont, CA, USA). TNF-α, IL-1β, and IL-6 enzyme-linked immunosorbent assay (ELISA) kits were purchased from BD Biosciences (Cambridge, MA, USA). ECL detection kit (34580) was obtained from Thermo Fisher Scientific (Waltham, MA USA). BSA (A0100–010) and protease inhibitor (P3100–010) were purchased from GenDEPOT (Katy, TX, USA). RIPA lysis buffer (RC2002–050-00) was purchased from Biosesang (Seongnam, Korea). QIAzol Lysis Reagent was purchased from Qiagen (79,306, Germantown, MD, USA). The following primary antibodies were used: antibodies against LC3BII (#2775) from Cell Signaling Technology (Danvers, MA, USA) and TFEB (A303-673 A) from Bethyl Laboratories, Inc. (Montgomery, TX, USA). Lamin B1 (#13435) and β-actin (A5441) were obtained from Invitrogen (San Diego, CA, USA) and used as internal controls. Horseradish peroxidase (HRP)-labeled secondary anti-mouse (#7076) and anti-rabbit (#7074) antibodies were purchased from Cell Signaling Technology. APC rats and anti-F4/80 antibodies (1:100, 566787) were obtained from BD Biosciences (San Jose, CA, USA). Anti-rabbit IgG Fab2 Alexa Fluor 488 molecular probes (1:2000, A-11070) were purchased as a secondary antibody from Invitrogen. (San Diego, CA, USA).

2.3. Cell culture

Murine macrophage RAW 264.7 cells (KCLB, Seoul, Korea) were seeded into 24-well plates (SPL Life Sciences, Pocheon, Korea) at a density of 5×10^4 cells per well and cultured at 37 °C in 1 mL of RPMI-1640 medium (Welgene, Daegu, Korea) supplemented with 10 % FBS and 1 % penicillin-streptomycin under a humidified 5 % CO_2 atmosphere. The cultured cells were stimulated with either 5 % CSE or 5 % and 15 % HTPE.

2.4. Preparation of CS extract and HTP aerosol extract

Commercial cigarettes and HTP used for aqueous smoke extract preparation were 3R4F reference cigarettes (Tobacco and Health Research Institute, University of Kentucky, USA) and iQOS cigarettes (Heets Green, Philip Morris, Korea), respectively. CSE and HTP aerosol extract (HTPE) were prepared as previously described (Chen et al., 2008; Panayiotidis et al., 2004; Wang et al., 2018). In brief, smoke from one cigarette or HTP unit was bubbled into 10 mL of RPMI-1640 using a peristaltic pump (VWR International, Radnor, PA, USA) at a constant flow rate for 5 min. The resulting CSE or HTPE was filtered through a 0.22 μm syringe filter (GVS Lifescience, Sanford, Maine, USA) to sterilize and remove insoluble particles. After filtration, 10 % FBS was added, defining the smoke from one cigarette or HTP in 10 mL RPMI-1640 as a 100 % CSE or HTPE solution.

2.5. Isolation and culture of mouse bone marrow-derived macrophages

Bone marrow-derived macrophages (BMMs) were isolated from BALB/c mice, as previously described (Weischenfeldt and Porse, 2008). Briefly, the femora and tibiae of the mice were removed aseptically and the marrow cavity was flushed with RPMI-1640 medium using a sterile 21-gauge needle. The resulting bone marrow suspension was washed twice and incubated with 30 ng/mL M-CSF (R&D Systems, Minneapolis, MN, USA) for 16 h. Thereafter, the floating cells were harvested and incubated for two days, which resulted in monocyte/macrophage-like cells that adhered to the culture plates. Adherent cells (BMMs) were collected after washing the plates with PBS.

2.6. Isolation of alveolar macrophages from the lungs

Alveolar macrophages (AMs) were isolated from the lungs of mice using the method described by van der Toorn et al. (2009). Bronchoalveolar lavage fluid (BALF) was collected by washing each lung three times with 1 mL of sterile PBS. The fluid was centrifuged at 200 $\times g$ for 5 min and a differential cell count was performed after washing the lavage cells. Lavage fluid from the mice lungs contained 98 % AMs, 96 % of which were viable, as determined using a trypan blue exclusion assay.

2.7. Cell viability assay

RAW 264.7 cells were cultured in a 96-well plate (SPL Life Sciences, Pocheon, Korea) at 3×10^4 cells per well and grown to 80 % confluency. The cells were then treated with CSE or HTPE at different concentrations (0, 5, 10, 15, 20, 30, and 40 %) and their viability was evaluated using the MTS assay, which was performed using CellTiter 96 aqueous one solution cell proliferation assay according to the manufacturer's instructions. The optical densities of the samples were determined at 490 nm using a spectrophotometer.

2.8. Intracellular reactive oxygen species measurement

The intracellular levels of ROS were evaluated using the fluorescent probe H_2DCFDA. After treating RAW 264.7 cells and BMMs with 5 % CSE or 5 % and 15 % HTPE for 15 h, the cells were briefly rinsed in PBS and incubated in a culture medium containing 5 μM H_2DCFDA at 37 °C for 30 min in the dark. Fluorescence was measured using FACSCanto II flow cytometer (BD Biosciences, San Jose, USA) and the data were analyzed using the FlowJo V10 software (Tree Star Inc., San Carlos, USA). To determine ROS levels using confocal microscopy, the cells were grown on glass coverslips in 24-well plates and stimulated with 5 % CSE or 5 % and 15 % HTPE for 15 h. After staining with 10 μM H_2DCFDA for 15 min, the coverslips were removed from the plate wells and analyzed on a slide using an Olympus FV1200 confocal microscope (Olympus, Tokyo, Japan).

2.9. Immunofluorescence technique

AMs were seeded onto sterile glass coverslips (Marienfeld, Lauda-Königshofen, Germany) in a 24-well plate at 5×10^4 cells per well and incubated in RPMI-1640 medium with 10 % FBS. The cells were stimulated with 5 % CSE for 24 h. The culture medium was removed from the coverslips and all cultured cells were fixed with 4 % ice-cold formaldehyde for 10 min and permeabilized with 0.2 % Triton X-100 (Sigma-Aldrich) in PBS. To reduce nonspecific staining, the samples were pre-blocked with 1 % bovine serum albumin (BSA) for 30 min at room temperature. The cells were then probed with anti-LC3BII antibody (1:100) and APC rat and anti-mouse F4/80 antibodies (1:100) overnight at 4 °C. Following this, the cells were analyzed using anti-rabbit IgG Fab2 Alexa Fluor® 488 molecular probes (1:2000). The immunofluorescence images were obtained using a confocal microscopy system (FV3000; Olympus Corporation, Shinjuku, Tokyo, Japan).

2.10. Stability analysis of housekeeping genes

The BestKeeper software (Pfaffl et al., 2004) was used for the stability analysis of the five housekeeping genes (HKGs; Actb, Gapdh, Hprt1, RPS3, and CYPA). The BestKeeper assessed the stability of index numeracy by analyzing the standard deviation (SD) and coefficient of variance (CV) for various expression values. The details regarding HKG primers are given in Supplementary Table 1.

2.11. RNA isolation and quantitative real-time polymerase chain reaction

Total RNA from cultured cells was extracted using QIAzol reagent and reverse-transcribed with random primers and M-MLV reverse transcriptase (Promega, Madison, USA). Quantitative real-time PCR (qPCR) was performed using SYBR Green Taq polymerase (Qiagen, Hilden, Germany) on a StepOnePlus Real-Time PCR System (Applied Biosystems, Foster City, CA, USA). The housekeeping gene 18S rRNA (RPS) was amplified in parallel with the genes of interest. The relative amount of transcript was calculated based on the $2^{-\Delta\Delta Ct}$ method. The following primers were used: 5′-GCC TCT TCT CAT TCC TGC TTG-3′ and 5′-CTG ATG AGA GGG AGG CCA TT-3′ (TNF-α); 5′-TGG ACC TTC CAG GAT GAG GAC A-3′ and 5′- GTT CAT CTC GGA GCC TGT AGT-3′ (IL-1β); 5′-TAC CAC TTC ACA AGT CGG AGG C-3′ and 5′-CTG CAA GTG CAT CAT CGT TGT TC-3′ (IL-6); 5′-CTG GTG AAA AGG ACC TCT CGA AG-3′ and 5′-CCA GTT TCA CTA ATG ACA CAA ACG-3′ (Hprt1).

2.12. Western blot analysis

RAW 264.7 cells and BMMs were lysed with RIPA lysis buffer and 1 % protease inhibitor mixture. After centrifugation for 15 min at 16,000 $\times g$, the supernatant was recovered. Typically, 20 μg of protein per lane was loaded on sodium dodecyl sulfate-polyacrylamide gel electrophoresis (SDS-PAGE) gels and transferred onto nitrocellulose membranes (Cytiva, Marlborough, USA). The membranes were blocked for 1 h with 5 % skimmed milk in PBS containing 0.05 % Tween 20 (PBS-T) and incubated overnight at 4 °C with primary antibodies against LC3BII, TFEB, Lamin B1, and β-actin. After washing with PBS-T, the membrane was incubated for 1 h with horseradish peroxidase-conjugated secondary antibodies and developed using the enhanced chemiluminescence (ECL) detection system (GE Healthcare, Waukesha, WI, USA).

2.13. Nuclear and cytosolic fractionation

To determine TFEB localization, RAW 264.7 cells were subjected to nuclear and cytosolic fractionation using a commercial kit following the manufacturer's instructions. Proteins were separated by SDS-PAGE and transferred onto nitrocellulose membranes. The membranes were blocked with 5 % skimmed milk in PBS containing 0.05 % Tween 20 (PBS-T) for 1 h at room temperature, followed by overnight incubation at 4 °C with primary TFEB, Lamin B1, and β-actin antibodies. After washing with 1× PBS-T, the membranes were incubated with horseradish peroxidase-conjugated secondary antibodies for 1 h at room temperature and developed using an ECL detection system (GE Healthcare).

2.14. Measurement of cytokines

The levels of cytokines in BALF obtained from mice or cell culture supernatants were determined using ELISA kits (R&D Systems) following the manufacturer's instructions.

2.15. Detection of acidic vesicular organelles

Acidic vesicular organelles (AVOs; autolysosomes) were stained with acridine orange (AO) as previously described (Thomé et al., 2016) and quantified using flow cytometry. The cells were stained with AO (1

μg/mL) for 20 min and then washed twice before being analyzed using flow cytometry.

2.16. Detection of oxidized TFEB via carboxymethylation

Subsequently, the medium was removed, and the cells were immediately frozen in liquid nitrogen. The lysis buffer containing 100 μM N-(biotinoyl)-N′-(iodoacetyl) ethylenediamine (BIAM) was deoxygenated by bubbling with nitrogen gas at a low flow rate for 20 min. The frozen cells were lysed in RIPA buffer containing a protease inhibitor, followed by incubation for 15 min at room temperature. The lysates were then clarified by centrifugation and immunoprecipitated with 1 μg of TFEB-specific antibody (Bethyl Laboratories). Immunocomplexes labeled with BIAM were detected using HRP-conjugated streptavidin and developed using an ECL detection system.

2.17. Autophagosome quantification

Autophagy analysis of RAW 264.7 cells was carried out using a Cyto-ID autophagy detection kit on glass coverslips in 24-well plates. RAW 264.7 cells were stimulated with either 5 % CSE or 5 %, 10 % and 15 % HTPE for 15 h. Following the manufacturer's instructions, the cells were stained with Cyto-ID Green dye and Hoechst 33342 at 37 °C for 30 min. The coverslips were then removed from the wells and placed on slides for confocal microscopy. Fluorescent images were analyzed using an Olympus FV1200 confocal microscope (Olympus, Tokyo, Japan).

2.18. Statistical analysis

All values were expressed as means ± standard error of the mean (SEM). Each series of experiments was repeated at least three times, and the sample means were normally distributed. Consequently, one-way analysis of variance (ANOVA) was employed for comparisons involving more than two groups, followed by Bonferroni post-hoc tests. *t*-tests were used for two-group comparisons. Statistical analysis was conducted using GraphPad Prism 5 (GraphPad Prism Software Inc., CA, USA) and SPSS 24.0 (SPSS Inc., IL, USA). A *p*-value less than 0.05 was considered statistically significant.

3. Results

3.1. Comparison of the cytotoxicity effects induced by iQOS aerosol and 3R4F extract

The cell viability was evaluated using the MTS assay. We compared the cytotoxicity of the iQOS aerosol and 3R4F extract in murine macrophage RAW 264.7 cells. iQOS-derived and 3R4F-derived extracts exhibited dose-dependent cytotoxicity in RAW264.7 cells (Fig. 1). Following exposure to 3R4F at concentrations of 5 % and 20 %, cell viability decreased to 37 % and 15 %, respectively. In contrast, exposure to 5 % and 15 % concentrations of HTPE resulted in higher viability levels of 64 % and 36 %, respectively. We observed a dose-dependent decrease in cell viability after administering CSE or HTPE. Specifically, we found that both 5 % CSE and 15 % HTPE resulted in a significant inhibitory effect, reducing RAW 264.7 cell viability to approximately 40 %. These concentrations were selected based on their notable impact on cell viability, which informed our in vitro assays. These results indicated that HTPE was less cytotoxic than the 3R4F extract.

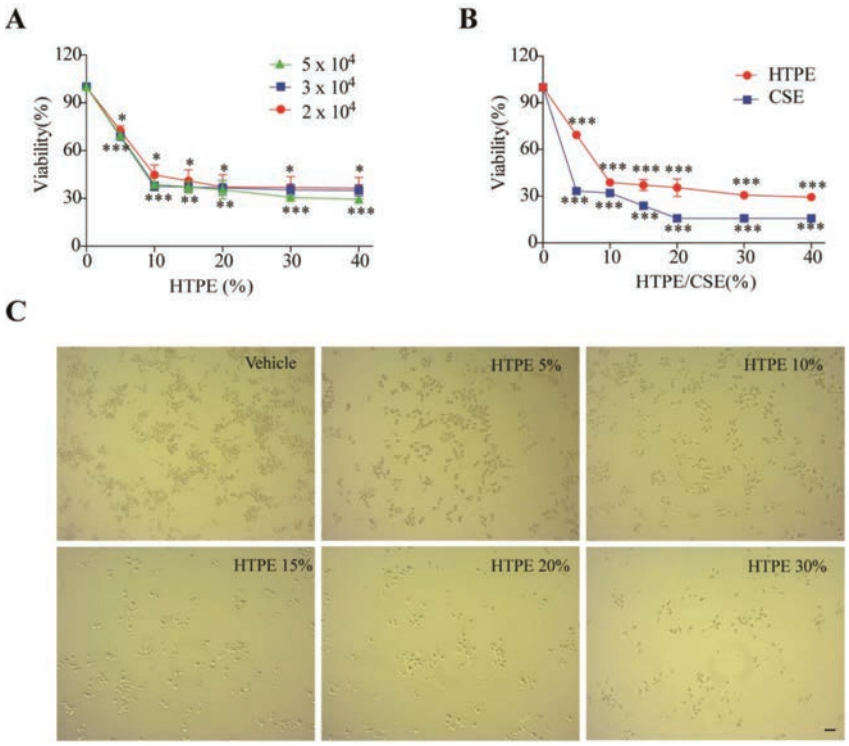

Fig. 1. Effect of heat-not-burn tobacco product extract (HTPE) and cigarette smoke extract (CSE) on the viability of RAW264.7 cells. (A) RAW 264.7 cells were seeded at varying densities in a 96-well plate and incubated with the indicated concentrations of the HTP for 24 h. (B) These cells were treated with HTPE or CSE at the various concentrations (0 %, 5 %, 10 %, 15 %, 20 %, 30 %, and 40 %) for 24 h. The cell viability was measured using the MTS assay. (C) Light microscopy of the cells cultured with HTPE in a medium for 24 h. Scale bar = 50 μm. Data are representative of three independent experiments. *$p < 0.05$, **$p < 0.01$, ***$p < 0.001$ compared with untreated cells.

3.2. Autophagy enhancement by HTP in macrophages

Given that our previous data demonstrated that CSE enhances autophagy in macrophages and that autophagy is closely associated with lung inflammation (Sul et al., 2023; Zhang et al., 2024), we hypothesized that HTP may increase autophagy, thus, affecting the inflammation of lung macrophages. We assessed autophagosome formation by immunoblotting cell lysates with an antibody against microtubule-associated protein light chain 3 (LC3) to determine whether the effects of HTP on macrophages were due to autophagy induction. As shown in Fig. 2A and B, HTP increased lipidated LC3B (LC3BII), a marker of autophagic flux in RAW 264.7, mouse macrophages, and BMMs, which are primary macrophages generated from bone marrow cells. In addition, NAC, a ROS scavenger, significantly reduced the extract-induced increase in LC3BII levels (Fig. 2A). ROS removal by NAC ameliorated ROS-induced autophagy, which indicates that oxidative stress mediates HTPE- or CSE-induced autophagy. Next, cells were exposed to 3-MA, which is an autophagosome inhibitor. The addition of 3-MA significantly decreased the HTPE-stimulated LC3BII level (Fig. 2B). Furthermore, we employed Cyto-ID® Green dye to detect autophagic vacuole accumulation and flux. As depicted in Fig. 2A, B, and C, HTP-induced autophagy was significantly higher in cells than in the control group. Interestingly, the cells also showed a markedly higher increase in CSE-induced autophagic flux (Fig. 2C). We also evaluated whether HTPE facilitated the formation of AVOs and autolysosomes. AVO formation was determined using flow cytometry employing pH-sensitive AO fluorescent dye. As illustrated in Fig. 2D, the percentage of cells with AVOs increased in a dose-dependent manner with 5 %, 10 %, and 15 % HTP.

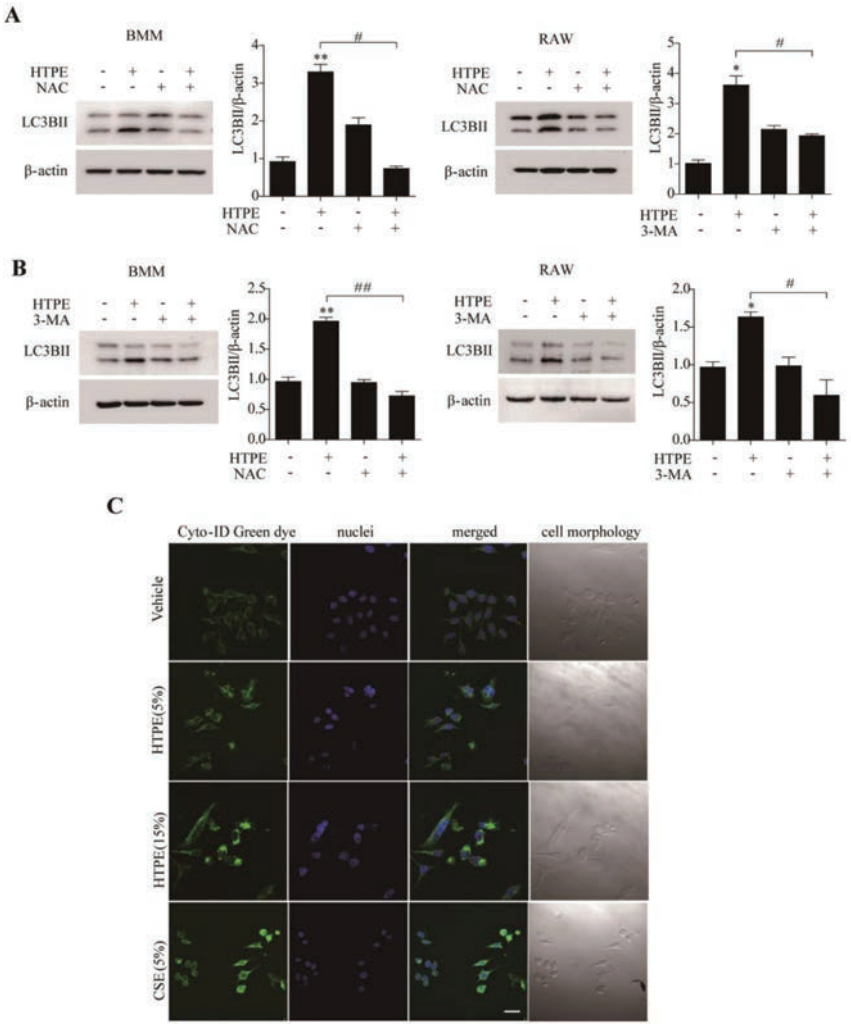

Fig. 2. Heat-not-burn tobacco product extract (HTPE) and cigarette smoke extract (CSE) induced autophagy in macrophage cells. RAW 264.7 cells and bone marrow-derived macrophages (BMMs) were treated with *N*-acetyl-l-cysteine (NAC; 5 mM) or 3-methyladenine (3-MA; 100 nM) for 1 h before adding HTPE. (A and B) After 24 h, the cell lysates were subjected to western blotting to determine LC3BII levels. The protein level of the autophagy marker, LC3BII, was assessed using immunoblotting in HTPE-treated cells compared with that in control cells. β-actin was used as a loading control for immunoblotting. (C) Autophagy was detected with the CYTO-ID® Green Detection Reagent 2. RAW264.7 cells treated with HTPE or CSE showed very bright green fluorescent signals and punctate structures. (D) Acridine orange (AO) staining was performed to detect acidic vesicular organelles (AVO). HTPE or CSE-induced AVO formation was analyzed using flow cytometry. As a positive control, cells were incubated without fetal bovine serum (FBS) for 4 h for starvation. The values represent the percentage of AVO-containing cells in representative experiments. (E) Alveolar macrophages from bronchoalveolar lavage fluid (BALF) of wild-type (WT) mice were treated with HTPE or CSE for 24 h. The cells were fixed and stained for LC3BII (green) and F4/80 (red) and were viewed under confocal microscope. Scale bars = 20 μm. Data are representative of three independent experiments. $^{*}p < 0.05$, $^{**}p < 0.01$, $^{***}p < 0.001$ compared with untreated cells. $^{\#}p < 0.05$, $^{\#\#}p < 0.01$ compared with CSE-treated cells. (For interpretation of the references to colour in this figure legend, the reader is referred to the web version of this article.)

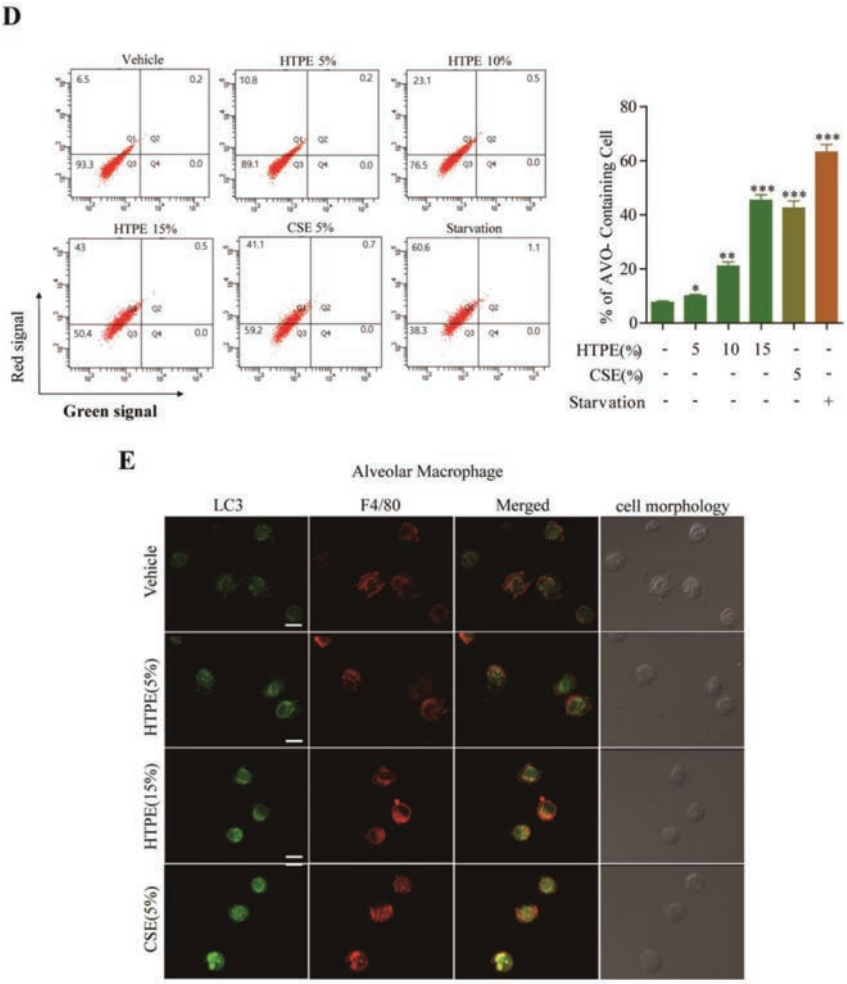

Fig. 2. (*continued*).

This outcome indicated that HTP promoted autophagy in macrophages and that HTPE triggered less autophagy than CSE. Starvation was also tested as a positive control for autophagy induction. Additionally, we isolated AMs from the mouse BALF. Subsequently, we performed double immunocytochemical staining for F4/80 (red) and LC3Bll (green) to investigate the HTP-induced autophagy in AMs. Compared with the control group, the activation of AM autophagy was higher in the HTPE group (Fig. 2E), although to a lesser extent than in the CSE group.

3.3. Oxidative stress induced by HTP in macrophages

As increased ROS has been reported to play a critical role in lung inflammation and diseases and to modulate autophagy in various cells (Scherz-Shouval et al., 2007; Chen et al., 2008), we hypothesized that ROS could be responsible for HTP-induced autophagy in lung macrophages. To evaluate whether HTP induced oxidative stress, we measured the cytoplasmic ROS production in HTPE- or CSE-treated cells using DCF-DA, which is oxidized to fluorescent DCF in the presence of ROS. HTPE treatment of RAW 264.7 cells resulted in significantly higher intracellular ROS production than that in the control group (Fig. 3A, B, and C). Similar patterns were observed for BMMs, in which an increase in cytoplasmic ROS levels was observed after HTPE or CSE treatment (Fig. 3D), suggesting that HTP exerts oxidant effects on macrophages.

3.4. Increased levels of TFEB-oxidizing ROS by HTP, leading to increased nuclear translocation of TFEB

ROS-induced oxidation of transcription factor EB (TFEB) facilitates its nuclear localization [7,30]. Thus, we sought to identify whether HTP could increase oxidized TFEB. As shown in Fig. 4A, HTP decreased the level of reduced TFEB, whereas NAC reversed the effect of HTP in decreasing the level of reduced TFEB. Next, we examined whether HTP increased TFEB nuclear translocation in macrophages, and whether ROS participated in this process. As shown in Fig. 4B, HTPE exposure increased the nuclear localization of TFEB. However, NAC reduced the HTP-induced increase in TFEB nuclear translocation, suggesting that high ROS levels trigger TFEB oxidation and contribute to an increase in TFEB nuclear translocation.

3.5. Lung inflammation induced by HTP-induced autophagy

Because previous studies have demonstrated that autophagy moderates the secretion of proinflammatory cytokines, including IL-1β (Sul et al., 2023), we investigated whether HTP-induced autophagy would increase inflammation, and whether inhibition of autophagy would reduce inflammation. First, RAW264.7 cells were stimulated with HTPE and CSE for 24 h. Expression levels of proinflammatory cytokines were determined using western blotting and RT-qPCR. As shown in Fig. 5A, CSE/HTPE treatment increased the secretion of TNF-α, IL-1β, and IL-6.

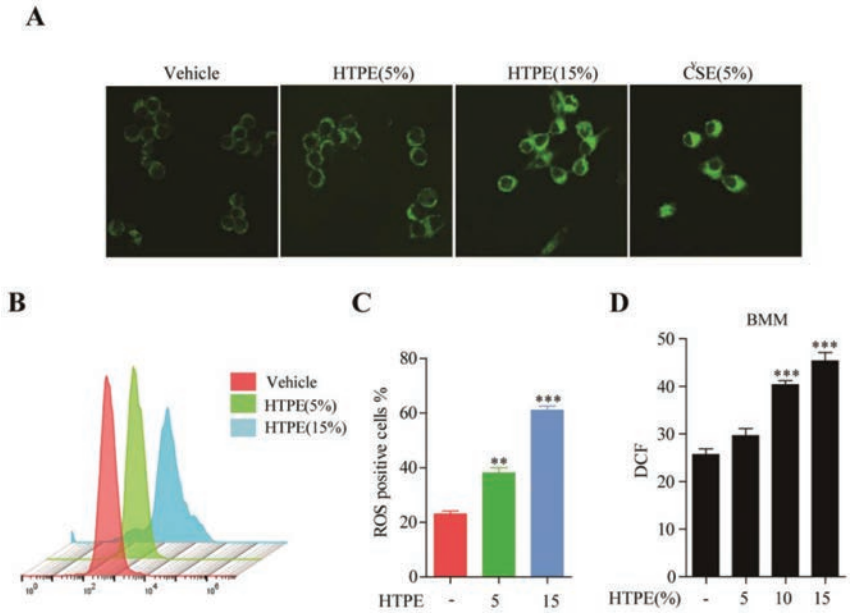

Fig. 3. Heat-not-burn tobacco product extract (HTPE) and cigarette smoke extract (CSE) induced oxidative stress in macrophages. RAW 264.7 cells, alveolar macrophages (AMs), and bone marrow-derived macrophages (BMMs) were treated with *N*-acetyl-l-cysteine (NAC; 5 mM) for 1 h and incubated with HTPE or CSE for 24 h. (A-B) Production of intracellular ROS in RAW 264.7 cells was determined using confocal microscopy and flow cytometry with H_2DCF-DA. Scale bar = 20 μm. (C) The values represent the percentage of reactive oxygen species (ROS)-positive cells in representative experiments. (D) Intracellular ROS level in BMM was determined using flow cytometry. Data are representative of three independent experiments. $^{**}p < 0.01$, $^{***}p < 0.001$ compared with untreated cells.

The stability of the candidate HKGs was assessed using BestKeeper, a commonly used algorithm for normalization and quantification. To evaluate the stability of the five candidate HKGs, several descriptive statistics, such as SD, CV, minimum (Min), and maximum (Max), were used in the BestKeeper analysis. We used the SD value from BestKeeper to rank the genes (Pfaffl et al., 2004; Vijayakumar and Sakuntala, 2024). Genes with lower SD values were considered more stable. BestKeeper identified Hprt1 as the most stable gene, followed by Actb, GAPDH, and RPS3. CYPA was ranked the least stable (Supplementary Table 2). Thus, Hprt1 was considered suitable for subsequent normalization of gene expression. In agreement with the data presented in Fig. 5A, RT-qPCR analysis showed that 5 % CSE stimulation significantly elevated the mRNA levels of TNF-α, IL-1β, and IL-6 compared with those in the control. Treatment with 10 % or 15 % HTPE increased the expression of these genes in RAW 264.7 cells, although to a lesser extent than that in the CSE group (Fig. 5B). However, ATG5 knockdown using siATG5 reduced the expression of the inflammatory cytokine IL-6 in the presence of HTPE (Fig. 5C). Loss of autophagy by siRNA silencing of ATG5 dramatically diminished the enhancing effect of HTPE on IL-6 secretion. Consistent with this result, the autophagy inhibitor 3-MA significantly decreased HTP-induced inflammatory cytokine expression (Fig. 5D).

4. Discussion

Our data demonstrated that HTP and 3R4F cigarette aerosols increased cytotoxicity in RAW 264.7 cells. These cigarette aerosols increased oxidative stress in RAW 264.7 cells, BMMs, and AMs. Additionally, oxidative stress triggered TFEB oxidation and induced its nuclear translocation, thereby ameliorating autophagy and inflammation in HTP- and 3R4F-exposed macrophages. Both HTP and 3R4F cigarettes had the same autophagy-induced lung inflammation, whereas exposure to the HTP aerosol showed lower in vitro cytotoxicity, oxidative stress, and inflammatory responses than conventional cigarettes.

The female rodents were selected for their susceptibility to smoke-induced damage and early onset of emphysema, providing a relevant model for studying tobacco exposure effects. We will highlight the relevance of this animal model, noting that its pathological features can help understand human health impacts. Additionally, while disease mechanisms differ across species, conserved biological processes can inform insights into human smoker sensitivities.

Several studies have demonstrated that heated tobacco products contain reduced levels of harmful constituents, such as nicotine, tar, carbon monoxide, and nitrosamines (Bekki et al., 2017; Farsalinos et al., 2018a). Dusautoir et al. (2021) compared the cytotoxicity of iQOS, burning cigarettes, and e-cigarettes in bronchial epithelial cells. The results indicated that HTPs could potentially cause less harm than tobacco cigarettes, but are more harmful than e-cigarettes. Consistent with these results, our study showed that lung macrophages were exposed to solutions prepared from the HTP and 3R4F to evaluate their cytotoxicity. Compared to 3R4F, HTPE exposure induced significantly higher cell viability at both 5 % and 20 % concentrations, indicating lower cytotoxicity.

Excessive ROS production can directly harm immune cells, such as macrophages and neutrophils, which secrete various inflammatory chemokines (Rahman et al., 2006). AMs play a crucial role in the pathogenesis of lung injury as they initiate inflammatory responses and facilitate neutrophil infiltration and tissue damage in the lungs (Franke-Ullmann et al., 1996). AMs have also been implicated in COPD pathogenesis. Recent studies have confirmed that CS-induced ROS production leads to oxidative stress, autophagy, and the production of inflammatory factors (Vij et al., 2018). iQOS aerosols can lead to a decline in mitochondrial reductase activity, subsequently resulting in increased production ROS and oxidative damage (Dröse, 2013; Korge et al., 2015). According to Wang et al. (2020b), although HTP-induced oxidative stress in macrophages is less than that induced by combustible cigarettes, both HnB products and combustible cigarettes decrease GSH and increase ROS levels, thereby suggesting that HnB products could enhance oxidative stress in macrophages. Consistent with these findings, our results also indicated that HTP aerosols induced intracellular ROS levels in macrophages, such as RAW264.7, BMMs, and AMs, but at lower

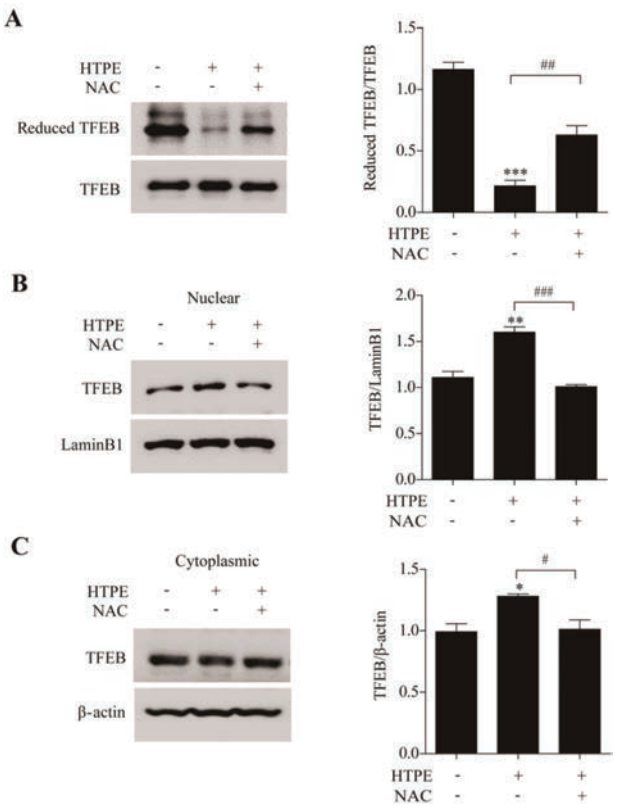

Fig. 4. Heat-not-burn tobacco product extract (HTPE) and cigarette smoke extract (CSE) increase the reactive oxygen species (ROS)-induced TFEB oxidation, and enhance its nuclear translocation. (A) The cell lysates were labeled with N-(biotinoyl)-N′-(iodoacetyl) ethylenediamine, and TFEB was immunoprecipitated from each sample. To assess the reduced form of TFEB, horseradish peroxidase (HRP)-streptavidin immunoblotting was used. (B and C) Western blot analysis of nuclear and cytoplasmic fractions from HTPE or CSE-treated cells using anti-TFEB antibodies. Expression levels were normalized to β-actin (cytoplasmic extract) or Lamin B1 (nuclear fraction). Data are representative of three independent experiments. $^{*}p < 0.05$, $^{**}p < 0.01$, $^{***}p < 0.001$ compared with untreated cells. $^{\#}p < 0.05$, $^{\#\#}p < 0.01$, $^{\#\#\#}p < 0.001$ compared with CSE-treated cells.

levels than did conventional cigarettes. Furthermore, previous studies have revealed that ROS are responsible for autophagy and that their activation in macrophages regulates early lung inflammation (Zhang et al., 2014).

Autophagy contributes to maintaining cellular homeostasis and is essential for cell survival. However, excessive autophagy can have detrimental effects leading to permanent lung damage. Studies have indicated that impaired autophagy hastens COPD progression, which suggests that it plays a protective role against CSE-induced COPD pathogenesis. However, other studies have reported that autophagy activation can negatively affect the prognosis of COPD (Gouzi et al., 2018; Wang et al., 2018). According to Wang et al. (2018), CSE-induced autophagy exacerbates lung damage in patients with COPD. Consistent with previous studies, exposure to aerosol extracts from HTP products and 3R4F cigarettes resulted in a significant increase in oxidative stress-induced autophagy, as demonstrated by the elevated levels of LC3II and the fraction of AVO-containing cells. In contrast, the inhibition of autophagy by 3-MA resulted in a decrease in the up-regulation of LC3II and the proportion of AVO-containing cells induced by cigarette aerosols in macrophages. To the best of our knowledge, few studies have reported the mechanisms underlying HTP-induced autophagy, and this is the first study to identify autophagy-related mechanisms in controlling lung inflammation. Moreover, we found that NAC, a ROS scavenger, reduced the increased levels of LC3II and AVO-containing cell fractions induced by HTP aerosols, indicating that increased ROS levels could mainly mediate HTP-induced autophagy. In addition, oxidative stress elevates DNA, lipid, and protein oxidation in the lungs and blood of patients with COPD (Doll, 1999). Wang et al. (2020a) showed that TFEB can be activated upon direct cysteine oxidation by ROS and regulates autophagy and lysosome biogenesis. In agreement with this, we found that ROS directly oxidizes TFEB and leads to its nuclear localization to enhance autophagy, which indicates that TFEB is a direct target of ROS. Given the established interactions among autophagy (Nivon et al., 2009), NF-κB signaling, and inflammation, assessing NF-κB phosphorylation could offer crucial insights into the underlying molecular mechanisms. However, the specific mechanisms by which NF-κB phosphorylation is involved in autophagy activation after cigarette exposure are still not fully understood, underscoring the necessity for further research in this area. Recent in vitro studies have demonstrated that the inhalation of iQOS aerosols has the potential to induce oxidative stress and inflammation (Bhat et al., 2021). iQOS aerosols caused damage and pro-inflammatory changes in the lungs, similar to those elicited by CS exposure. In contrast, previous studies indicated that HTPs produced lower proinflammatory cytokines, including IL-6, IL-1β, and TNFα, in different lung cell lines than did conventional cigarettes (Dusautoir et al., 2021; Lyu et al., 2022). Additionally, our findings indicated that HTPE causes the secretion of IL-6, IL-1β, and TNFα (Fig. 2E-J), although to a lesser extent than does CSE, thereby suggesting a partially elicited inflammatory response.

Cigarette smoke (CS) exposure can lead to macrophage reprogramming and disrupt the M1/M2 balance (Gleeson et al., 2018). This exposure is linked to a mixed cellular phenotype, with M1 characteristics indicated by an increased frequency of CD80. Conversely, CS has also been shown to elevate markers of the M2 phenotype, which are associated with dysregulated inflammation. For instance, Zhang et al. demonstrated that the number of CD206+ LC3B+ cells was significantly higher in the COPD group compared to the control group. Furthermore, macrophages exposed to heated tobacco products (HTPs) exhibit an increased frequency of the M2 marker CD163 (Scharf et al., 2024). Analyzing macrophage polarization is crucial to determine if HTPs skew responses toward M1 or M2 phenotypes, providing insights into inflammatory pathways. Thus, further investigation in future experiments is necessary. This study presents some limitations. First, the authors have not conducted dosimetry on the extracts. Especially, quantifying nicotine in fresh extracts is essential for understanding cell applications and confirming trapping efficiency, necessitating further experiments. Second, filtration was performed to eliminate bacterial contamination in in vitro cell cultures, allowing the removal of insoluble particles. Consequently, the authors are unable to assess whether this process also affects the biological activity of the extracts by removing important hydrophobic or particulate components. HTPs are designed to deliver nicotine while reducing harmful constituents, potentially allowing adult smokers to achieve satisfaction similar to that of traditional cigarettes and transition to a less harmful alternative. Additionally, the material captured as tar in HTP aerosols differs compositionally from the tar present in cigarette smoke. Several studies indicate that HTPs have lower levels of substances like tar, carbon monoxide, and nitrosamines (Bekki et al., 2017; Farsalinos et al., 2018b; Dusautoir et al., 2021). The nicotine content in HTP aerosol ranges from 0.5 to 1.50 mg per cigarette, which is lower than the 0.7 to 2.1 mg found in traditional cigarettes (World Health Organization, 2020). On the other side, some research shows comparable nicotine levels between HTP aerosol and traditional smoke (1R5F, 3R4F; Bekki et al., 2017; Li et al., 2019).” However, the use of nicotine poses risks for adults as well (Centers for Disease Control and Prevention, 2020). Further independent and long-term research is essential to assess the safety of HTP tobacco products.

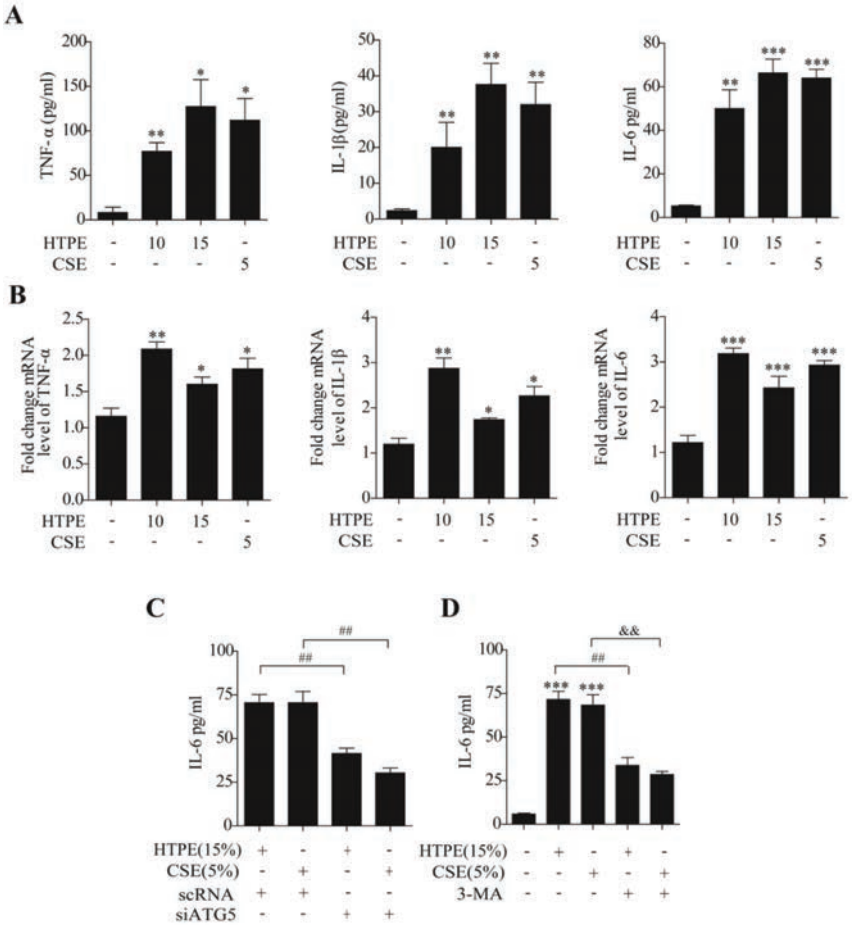

Fig. 5. Heat-not-burn tobacco product extract (HTPE) and cigarette smoke extract (CSE) upregulate autophagy-induced lung inflammation. RAW 264.7 cells were stimulated with HTPE or CSE for 24 h. (A and B) The conditioned supernatants were harvested, and secreted levels of TNF-α, IL-1β, and IL-6 were assessed using ELISA and RT-qPCR. Hprt1 was used as the housekeeping gene for normalization. (C) RAW 264.7 cells were transfected with scRNA or siATG5 and incubated further with HTPE or CSE (10 μM) for 24 h. (D) RAW 264.7 cells were treated with 3-MA (3-methyladenine; 100 nM) for 1 h, followed by addition of HTPE or CSE. $^{*}p < 0.05$, $^{**}p < 0.01$, $^{***}p < 0.001$ compared with untreated cells. $^{\#\#}p < 0.01$ compared with scRNA-treated cells. $^{\&\&}p < 0.01$ with each corresponding control.

In conclusion, our study demonstrated that aerosols from HTP and 3R4F cigarettes increased the cytotoxicity in macrophages. Exposure to cigarette aerosols increased oxidative stress, which in turn triggered TFEB oxidation and promoted its nuclear translocation. TFEB oxidation by ROS subsequently led to enhanced autophagy and inflammatory responses in macrophages exposed to either HTP or 3R4F aerosols. Notably, exposure to HTP aerosols induced lower levels of cytotoxicity, oxidative stress, and inflammation compared to conventional cigarette aerosols in vitro. However, the potential harmful effects of HTP remain a subject of debate, and further studies are required to elucidate their health impacts as an alternative to conventional cigarettes, both in vitro and in vivo. The findings may provide valuable insights into the inflammatory processes associated with both COPD and other smoking-related diseases, such as cardiovascular disease.

CRediT authorship contribution statement

Ok Joo Sul: Writing – original draft, Visualization, Resources, Methodology, Data curation. **Hye Won Choi:** Methodology, Formal analysis, Data curation. **Seo Hee Park:** Methodology, Formal analysis, Data curation. **Min Ju Kim:** Methodology, Formal analysis, Data curation. **Seung Won Ra:** Writing – review & editing, Writing – original draft, Visualization, Supervision, Project administration, Funding acquisition, Conceptualization.

Funding

This work was financially supported by an Ulsan University Hospital Research Grant (2024-UUHBRI-01) and Basic Science Research Programs (2021R1I1A1A0104430413, 2022R1F1A106275312) of the National Research Foundation of Korea.

Declaration of competing interest

All authors listed have contributed to the work, approved, and agreed to submit the manuscript to *Toxicology* in Vitro. All authors agree to accept complete responsibility for the contents of the manuscript. No significant amount of data reported in this manuscript has been published or is under consideration for publication elsewhere. All authors disclose any conflict of interest.

Appendix A. Supplementary data

Supplementary data to this article can be found online at https://doi.org/10.1016/j.tiv.2025.106151.

Data availability

Data will be made available on request.

References

Bekki, K., Inaba, Y., Uchiyama, S., Kunugita, N., 2017. Comparison of chemicals in mainstream smoke in heat-not-burn tobacco and combustion cigarettes. J. UOEH 39, 201–207.

Bhat, T.A., Kalathil, S.G., Leigh, N., Muthumalage, T., Rahman, I., Goniewicz, M.L., Thanavala, Y.M., 2021. Acute effects of heated tobacco product (IQOS) aerosol inhalation on lung tissue damage and inflammatory changes in the lungs. Nicotine Tob. Res. 23, 1160–1167.

Centers for Disease Control and Prevention, 2020. Heated Tobacco Products. Available online: https://www.cdc.gov/tobacco/basic_information/heated-tobacco-products/ (accessed 18 Mar. 2023).

Chen, Z.H., Kim, H.P., Sciurba, F.C., Lee, S.J., Feghali-Bostwick, C., Stolz, D.B., Dhir, R., Landreneau, R.J., Schuchert, M.J., Yousem, S.A., Nakahira, K., Pilewski, J.M., Lee, J. S., Zhang, Y., Ryter, S.W., Choi, A.M., 2008. Egr-1 regulates autophagy in cigarette smoke-induced chronic obstructive pulmonary disease. PLoS One 3, e3316.

Chen, Y., McMillan-Ward, E., Kong, J., Israels, S.J., Gibson, S.B., 2008. Oxidative stress induces autophagic cell death independent of apoptosis in transformed and cancer cells. Cell Death Differ. 15, 171–182.

Christenson, S.A., Smith, B.M., Bafadhel, M., Putcha, N., 2022. Chronic obstructive pulmonary disease. Lancet 399, 2227–2242.

De Cunto, G., Bartalesi, B., Cavarra, E., Balzano, E., Lungarella, G., Lucattelli, M., 2018. Ongoing lung inflammation and disease progression in mice after smoking cessation: beneficial effects of formyl-peptide receptor blockade. Am. J. Pathol. 188, 2195–2206.

Doll, R., 1999. Risk from tobacco and potentials for health gain. Int. J. Tuberc. Lung Dis. 3, 90–99.

Dröse, S., 2013. Differential effects of complex II on mitochondrial ROS production and their relation to cardioprotective pre- and postconditioning. Biochim. Biophys. Acta 1827, 578–587.

Dusautoir, R., Zarcone, G., Verriele, M., Garçon, G., Fronval, I., Beauval, N., Allorge, D., Riffault, V., Locoge, N., Lo-Guidice, J.M., Anthérieu, S., 2021. Comparison of the chemical composition of aerosols from heated tobacco products, electronic cigarettes and tobacco cigarettes and their toxic impacts on the human bronchial epithelial BEAS-2B cells. J. Hazard. Mater. 401, 123417.

Farsalinos, K.E., Yannovits, N., Sarri, T., Voudris, V., Poulas, K., 2018a. Nicotine delivery to the aerosol of a heat-not-burn tobacco product: comparison with a tobacco cigarette and E-cigarettes. Nicotine Tob. Res. 20, 1004–1009.

Farsalinos, K.E., Yannovits, N., Sarri, T., Voudris, V., Poulas, K., Leischow, S.J., 2018b. cigarette and a tobacco cigarette. Addiction 113, 2099–2106.

Finkelstein, J., Cha, E., Scharf, S.M., 2009. Chronic obstructive pulmonary disease as an independent risk factor for cardiovascular morbidity. Int. J. Chron. Obstruct. Pulmon. Dis. 4, 337–349.

Franke-Ullmann, G., Pförtner, C., Walter, P., Steinmüller, C., Lohmann-Matthes, M.L., Kobzik, L., 1996. Characterization of murine lung interstitial macrophages in comparison with alveolar macrophages in vitro. J. Immunol. 157, 3097–3104.

Gan, W.Q., Man, S.F., Postma, D.S., Camp, P., Sin, D.D., 2006. Female smokers beyond the perimenopausal period are at increased risk of chronic obstructive pulmonary disease: a systematic review and meta-analysis. Respir. Res. 7, 52.

Glantz, S.A., 2018. Heated tobacco products: the example of IQOS. Tob. Control. 27, s1–s6.

Gleeson, L.E., O'Leary, S.M., Ryan, D., McLaughlin, A.M., Sheedy, F.J., Keane, J., 2018. Cigarette smoking impairs the bioenergetic immune response to mycobacterium tuberculosis infection. Am. J. Respir. Cell Mol. Biol. 59, 572–579.

Gouzi, F., Blaquière, M., Catteau, M., Bughin, F., Maury, J., Passerieux, E., Ayoub, B., Mercier, J., Hayot, M., Pomiès, P., 2018. Oxidative stress regulates autophagy in cultured muscle cells of patients with chronic obstructive pulmonary disease. J. Cell. Physiol. 233, 9629–9639.

Hodge, S., Matthews, G., Mukaro, V., Ahern, J., Shivam, A., Hodge, G., Holmes, M., Jersmann, H., Reynolds, P.N., 2011. Cigarette smoke-induced changes to alveolar macrophage phenotype and function are improved by treatment with procysteine. Am. J. Respir. Cell Mol. Biol. 44, 673–681.

Horinouchi, T., Miwa, S., 2021. Comparison of cytotoxicity of cigarette smoke extract derived from heat-not-burn and combustion cigarettes in human vascular endothelial cells. J. Pharmacol. Sci. 147, 223–233.

Joo Sul, O., Won Choi, H., Won Ra, S., 2024. Grape seed proanthocyanidin extract modulates cigarette smoke extract-induced epithelial cell apoptosis by inhibiting oxidative stress in chronic obstructive pulmonary disease. J. Funct. Foods 112, 105907.

Katanoda, K., Yako-Suketomo, H., 2012. Mortality attributable to tobacco by selected countries based on the WHO global report. Jpn. J. Clin. Oncol. 42, 561–562.

Korge, P., Calmettes, G., Weiss, J.N., 2015. Increased reactive oxygen species production during reductive stress: the roles of mitochondrial glutathione and thioredoxin reductases. Biochim. Biophys. Acta 1847, 514–525.

Langhammer, A., Johnsen, R., Gulsvik, A., Holmen, T.L., Bjermer, L., 2003. Sex differences in lung vulnerability to tobacco smoking. Eur. Respir. J. 21, 1017–1023.

Leigh, N.J., Tran, P.L., O'Connor, R.J., Goniewicz, M.L., 2018. Cytotoxic effects of heated tobacco products (HTP) on human bronchial epithelial cells. Tob. Control. 27, s26–s29.

Li, X., Luo, Y., Jiang, X., Zhang, H., Zhu, F., Hu, S., Hou, H., Hu, Q., Pang, Y., 2019. Chemical analysis and simulated pyrolysis of tobacco heating system 2.2 compared to conventional cigarettes. Nicotine Tob. Res. 21, 111–118.

Lyu, Q., Jiang, L., Zheng, H., Hayashi, S., Sato, K., Toyokuni, S., 2022. Diluted aqueous extract of heat-not-burn tobacco product smoke causes less oxidative damage in fibroblasts than conventional cigarette. J. Clin. Biochem. Nutr. 71, 55–63.

March, T.H., Wilder, J.A., Esparza, D.C., Cossey, P.Y., Blair, L.F., Herrera, L.K., McDonald, J.D., Campen, M.J., Mauderly, J.L., Seagrave, J., 2006. Modulators of cigarette smoke-induced pulmonary emphysema in A/J mice. Toxicol. Sci. 92, 545–559.

National Research Council (US), 2011. Committee for the Update of the Guide for the Care and Use of Laboratory Animals. Guide for the Care and Use of Laboratory Animals, 8th edition. National Academies Press, Washington, DC.

Nivon, M., Richet, E., Codogno, P., Arrigo, A.P., Kretz-Remy, C., 2009. Autophagy activation by NFkappaB is essential for cell survival after heat shock. Autophagy 5, 766–783.

Panayiotidis, M.I., Stabler, S.P., Allen, R.H., Ahmad, A., White, C.W., 2004. Cigarette smoke extract increases S-adenosylmethionine and cystathionine in human lung epithelial-like (A549) cells. Chem. Biol. Interact. 147, 87–97.

Pfaffl, M.W., Tichopad, A., Prgomet, C., Neuvians, T.P., 2004. Determination of stable housekeeping genes, differentially regulated target genes and sample integrity: BestKeeper–Excel-based tool using pair-wise correlations. Biotechnol. Lett. 26, 509–515.

Rahman, I., Biswas, S.K., Kode, A., 2006. Oxidant and antioxidant balance in the airways and airway diseases. Eur. J. Pharmacol. 533, 222–239.

Sawa, M., Ushiyama, A., Inaba, Y., Hattori, K., 2022. Increased oxidative stress and effects on inflammatory cytokine secretion by heated tobacco products aerosol exposure to mice. Biochem. Biophys. Res. Commun. 610, 43–48.

Scharf, P., Sandri, S., Borges, P.P., Franco de Oliveira, T., Farsky, S.H.P., 2024. A single and short exposure to heated tobacco vapor or cigarette smoke affects macrophage activation and polarization. Toxicology 506, 153859.

Scherz-Shouval, R., Shvets, E., Fass, E., Shorer, H., Gil, L., Elazar, Z., 2007. Reactive oxygen species are essential for autophagy and specifically regulate the activity of Atg4. EMBO J. 26, 1749–1760.

Sohal, S.S., Eapen, M.S., Naidu, V.G.M., Sharma, P., 2019. IQOS exposure impairs human airway cell homeostasis: direct comparison with traditional cigarette and e-cigarette. ERJ Open Res. 5.

Sul, O.J., Choi, H.W., Oh, J., Ra, S.W., 2023. GSPE attenuates CSE-induced lung inflammation and emphysema by regulating autophagy via the reactive oxygen species/TFEB signaling pathway. Food Chem. Toxicol. 177, 113795.

Thomé, M.P., Filippi-Chiela, E.C., Villodre, E.S., Migliavaca, C.B., Onzi, G.R., Felipe, K.B., Lenz, G., 2016. Ratiometric analysis of acridine orange staining in the study of acidic organelles and autophagy. J. Cell. Sci. 129, 4622–4632.

van der Toorn, M., Rezayat, D., Kauffman, H.F., Bakker, S.J., Gans, R.O., Koëter, G.H., Choi, A.M., van Oosterhout, A.J., Slebos, D.J., 2009. Lipid-soluble components in cigarette smoke induce mitochondrial production of reactive oxygen species in lung epithelial cells. Am. J. Phys. Lung Cell. Mol. Phys. 297, L109–L114.

Vij, N., Chandramani-Shivalingappa, P., Van Westphal, C., Hole, R., Bodas, M., 2018. Cigarette smoke-induced autophagy impairment accelerates lung aging, COPD-emphysema exacerbations and pathogenesis. Am. J. Phys. Cell Phys. 314, 73–87.

Vijayakumar, S., Sakuntala, M., 2024. Validation of reference gene stability for normalization of RT-qPCR in Phytophthora capsici Leonian during its interaction with Piper nigrum L. Sci. Rep. 14, 7331.

Wang, Y., Liu, J., Zhou, J.S., Huang, H.Q., Li, Z.Y., Xu, X.C., Lai, T.W., Hu, Y., Zhou, H.B., Chen, H.P., Ying, S.M., Li, W., Shen, H.H., Chen, Z.H., 2018. MTOR suppresses cigarette smoke-induced epithelial cell death and airway inflammation in chronic obstructive pulmonary disease. J. Immunol. 200, 2571–2580.

Wang, H., Wang, N., Xu, D., Ma, Q., Chen, Y., Xu, S., Xia, Q., Zhang, Y., Prehn, J.H.M., Wang, G., Ying, Z., 2020a. Oxidation of multiple MiT/TFE transcription factors links oxidative stress to transcriptional control of autophagy and lysosome biogenesis. Autophagy 16, 1683–1696.

Wang, L., Liu, X., Chen, L., Liu, D., Yu, T., Bai, R., Yan, L., Zhou, J., 2020b. Harmful chemicals of heat not burn product and its induced oxidative stress of macrophages at air-liquid interface: comparison with ultra-light cigarette. Toxicol. Lett. 331, 200–207.

Wang, H., Lu, F., Tian, Y., Zhang, S., Han, S., Fu, Y., Li, J., Feng, P., Shi, Z., Chen, H., Hou, H., 2024. Evaluation of toxicity of heated tobacco products aerosol and cigarette smoke to BEAS-2B cells based on 3D biomimetic chip model. Toxicol. in Vitro 94, 105708.

Weischenfeldt, J., Porse, B., 2008. Bone marrow-derived macrophages (BMM): isolation and applications. CSH Protoc. 2008 pdb.prot5080.

World Health Organization, 2020. Heated Tobacco Products—A Brief. Available online: https://apps.who.int/iris/bitstream/handle/10665/350470/WHO-EURO-2020-4571-44334-64934-eng.pdf?sequence=3&isAllowed=y (accessed 19 Apr. 2023).

Yoshida, T., Tuder, R.M., 2007. Pathobiology of cigarette smoke-induced chronic obstructive pulmonary disease. Physiol. Rev. 87, 1047–1082.

Zhang, H., Lei, Y., Yuan, P., Li, L., Luo, C., Gao, R., Tian, J., Feng, Z., Nice, E.C., Sun, J., 2014. ROS-mediated autophagy induced by dysregulation of lipid metabolism plays a protective role in colorectal cancer cells treated with gambogic acid. PLoS One 9, e96418.

Zhang, L., Cheng, T., Liu, C., He, S., Lu, J., 2024. The role and mechanism of macrophage autophagy in the experimental model of chronic obstructive pulmonary disease. Tob. Induc. Dis. 22.